REPORT DOCUMENTATION PAGE	Form Approved OMB No. 0704-0188

PLEASE DO NOT RETURN YOUR FORM TO THE ABOVE ADDRESS.

1. REPORT DATE *(DD-MM-YYYY)*	2. REPORT TYPE	3. DATES COVERED *(From - To)*
26112013	Final Technical Report	01 May 2010 - 31 Aug 2013

4. TITLE AND SUBTITLE
Slamming Testing of Facetted Bottom

5a. CONTRACT NUMBER

5b. GRANT NUMBER
N00014-10-1-0767

5c. PROGRAM ELEMENT NUMBER

6. AUTHOR(S)
Grenestedt, Joachim

5d. PROJECT NUMBER

5e. TASK NUMBER

5f. WORK UNIT NUMBER

7. PERFORMING ORGANIZATION NAME(S) AND ADDRESS(ES)
Lehigh University
526 Brodhead Avenue
Bethlehem, PA 18015

8. PERFORMING ORGANIZATION REPORT NUMBER

9. SPONSORING/MONITORING AGENCY NAME(S) AND ADDRESS(ES)
Office of Naval Research, 230 South Dearborn, Room 380, Chicago, IL 60604-1595
Defense Technical Information Center, 8725 John J Kingman Rd, Ste 0944, Fort Belvoir, VA 22060-6128
Naval Research Laboratory, 4555 Overlook Ave SW, Washington, DC 20375-5320

10. SPONSOR/MONITOR'S ACRONYM(S)
ONR

11. SPONSOR/MONITOR'S REPORT NUMBER(S)

12. DISTRIBUTION/AVAILABILITY STATEMENT
Statement A: Approved for public release; distribution is unlimited

13. SUPPLEMENTARY NOTES

14. ABSTRACT

The highest loads on bottoms of fast craft are due to slamming, or hydrodynamic impact. A 9 meter long steel / composite hybrid slamming load test facility has been employed for the purpose of furthering understanding of the slamming phenomenon. This craft is heavily instrumented with strain gages, accelerometers, cameras, an inertial navigation system and more. It has been subjected to tests in a lab environment, in calm seas, and in rough seas. Slamming tests were performed in the Atlantic Ocean at places such as off the coast of Barnegat Light, NJ. During these tests the boat was operated in sea state 3 at speeds of roughly 25 m/s. The data collected have been used to compare the behavior of the different bottom panels of the hull. In particular the response of starboard and port panels with different structural properties were compared, using time response, frequency spectra, peak counting, etc.

15. SUBJECT TERMS
Slamming, hydrodynamic impact, boat bottom, experimental fluid dynamics, ocean testing

16. SECURITY CLASSIFICATION OF:			17. LIMITATION OF ABSTRACT	18. NUMBER OF PAGES	19a. NAME OF RESPONSIBLE PERSON
a. REPORT	b. ABSTRACT	c. THIS PAGE	UU	19	Joachim Grenestedt
					19b. TELEPHONE NUMBER *(Include area code)* 610-758-4129

Standard Form 298 (Rev. 8/98)
Prescribed by ANSI Std. Z39.18

Contract Information

Contract Number	N000141-01-07-6-7
Title of Research	Slamming Testing of Facetted Bottom
Principal Investigator	Joachim L. Grenestedt
Organization	Lehigh University

Technical Section

Introduction

The highest loads on bottoms of fast craft are due to slamming, or hydrodynamic impact. A 9 meter long steel / composite hybrid slamming load test facility has been employed for the purpose of furthering understanding of the slamming phenomenon. This craft is heavily instrumented with strain gages, accelerometers, cameras, an inertial navigation system and more. It has been subjected to tests in a lab environment, in calm seas, and in rough seas. Slamming tests were performed in the Atlantic Ocean at places such as off the coast of Barnegat Light, NJ. During these tests the boat was operated in sea state 3 at speeds of roughly 25 m/s. The data collected have been used to compare the behavior of the different bottom panels of the hull.

Figure 1: The "Numerette" Slamming Load Test Facility

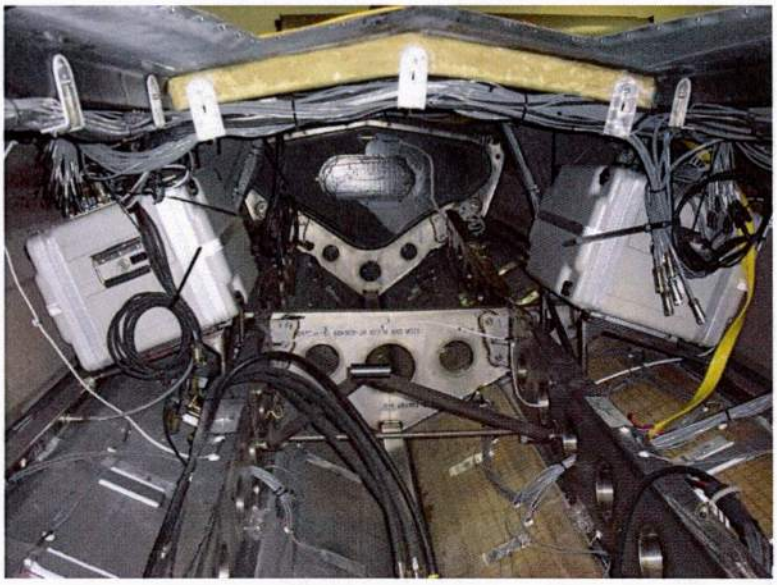

Figure 2: Onboard Instrumentation

Slamming Test Severity

During slamming tests accelerations were measured at bulkheads and on panels. Vertical accelerations at bulkheads were observed in excess of 40g and nearly 200g in bottom panels. Figure 3 shows the vertical acceleration at a bulkhead near the front of the boat during a typical slamming event, while Figure 4 shows vertical acceleration at a bulkhead near the rear of the boat. Using a low pass filter, the rigid body acceleration of the boat can be estimated. Figure 3 and Figure 4 have both 10 Hz and 50 Hz low pass filters plotted in addition to the original unfiltered data. The 10 Hz filter has been suggested for use in characterizing rigid body acceleration in slamming, but in this case it appears to not adequately resolve the rigid body motion. The 50 Hz lowpass attenuates the bulkhead vibration while presumably retaining the rigid body accelerations.

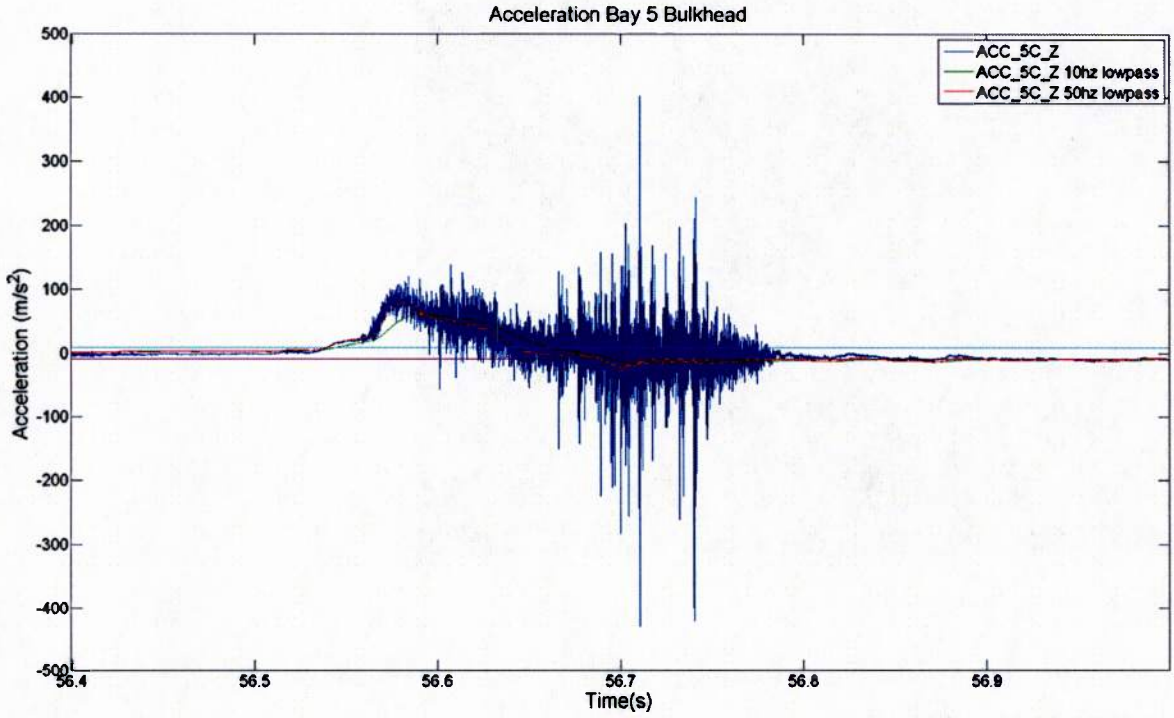

Figure 3: Bay 5 Bulkhead Vertical Acceleration, unfiltered and 10, 50 Hz Lowpass

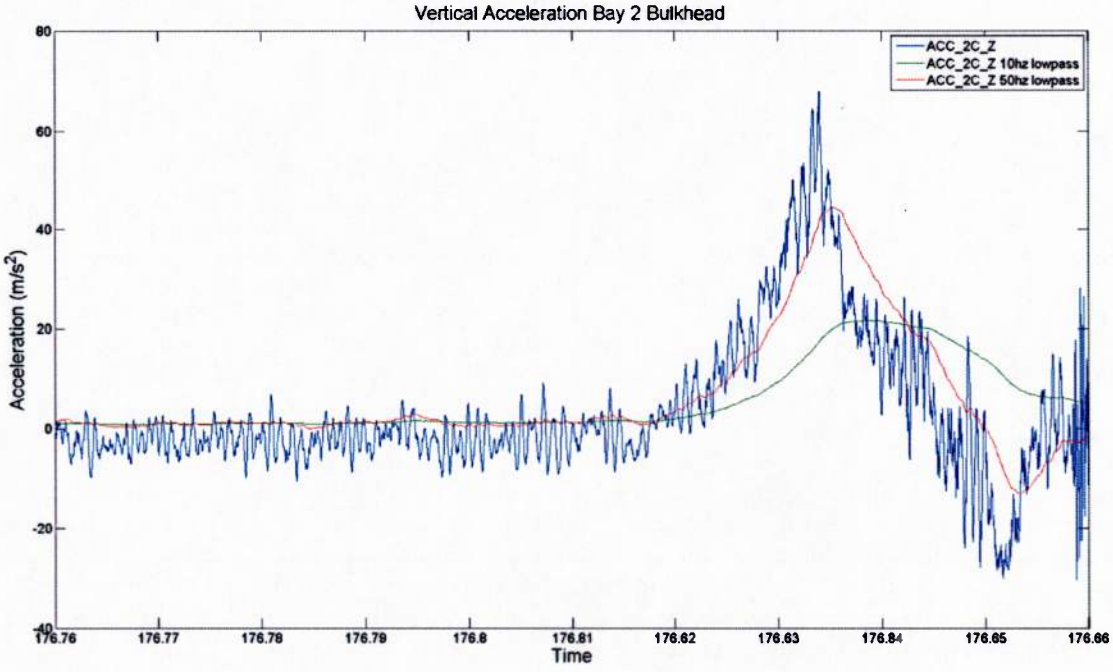

Figure 4: Bay 2 Bulkhead Vertical Acceleration, unfiltered and 10, 50 Hz Lowpass

For comparative purposes the intensity of slamming during some period can be described by a peak counting method. In this method, accelerations above an RMS value and separated in time by more than 0.5 seconds are identified as peaks. Figure 5 is an example of a 10 second time history of the LCG vertical acceleration with a low pass filter and all acceleration peaks identified by a red triangle. Table 1 and Table 2 show the A(1/n) accelerations at bulkheads near the bow and stern as well as the LCG for 10 Hz and 50 Hz low pass filtered time histories.

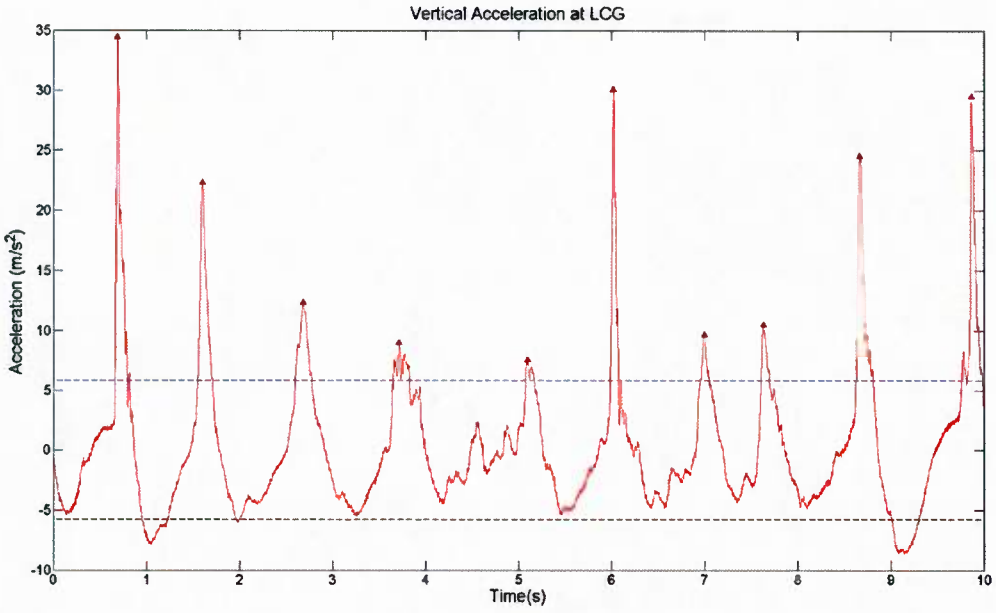

Figure 5: Vertical Acceleration at Longitudinal Center of Gravity

Table 1: A(1/n) Accelerations for 10Hz Low Pass Signal

	Bulkhead2 Vertical (g)	Bulkhead 5 Vertical (g)	LCG Vertical (g)
$A_{1/100}$	2.51	7.98	3.48
$A_{1/10}$	2.03	7.00	2.86
$A_{1/3}$	1.47	5.03	2.10

Table 2: A(1/n) Accelerations for 50Hz Low Pass Signal

	Bulkhead2 Vertical (g)	Bulkhead 5 Vertical (g)	LCG Vertical (g)
$A_{1/100}$	4.03	13.04	5.42
$A_{1/10}$	2.65	9.98	3.85
$A_{1/3}$	1.83	6.58	2.59

Facetted bottom panels

The facetted bottom of the slamming load test facility consists of ten separate foam core composite composite sandwich panels. Each of these panels has a different construction to allow for a comparative analysis. Figure 6 illustrates the general layup of each panel. The foam core used in all ten panels is the same, but the inner and outer skins have differing types, amounts and orientations of the reinforcements. The construction of the panels is detailed in

Table 3. The results presented here will focus on the behavior of the port and starboard panels in bay 4 of the craft, as identified in Figure 7.

Starboard and port bottom panels in Bay 4 have identical construction with the exception of fiber orientation of the carbon reinforcements. In the starboard panel there is more fiber oriented transverse or perpendicular to the keel (90 degree), whereas in the port panel there is more fiber oriented longitudinal or parallel to the keel (0 degree). The unsupported areas of the bottom panels are 4 times as long as they are wide so it is anticipated that the starboard panel will be substantially stiffer under an evenly distributed static loading. The objective of recent tests has been to relate this static performance to the panel response under slamming conditions. An upcoming publication will detail the background, experimental methodology and data analysis methods as well as results for panels in bays 2 and 3.

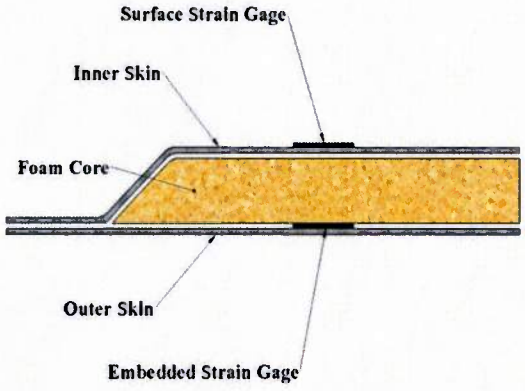

Figure 6: Composite Panel Construction and Instrumentation

Table 3: Composite Bottom Panel Construction

	Bay 1	Bay 2	Bay 3	Bay 4	Bay 5
Port	DB240 (±45°) 2 top layers Foam core 3 bottom layers 0° parallel	DBL700(0°, ±45°) 2 top layers Foam core 3 bottom layers 1 layer unidirectional 0° perpendicular	DBL700 (0°, ±45°) 2 top layers Foam core 3 bottom layers 1 layer unidirectional 0° perpendicular	DBL700(0°, ±45°) 2 top layers Foam core 3 bottom layers 1 layer unidirectional 0° parallel	DBL700(0°, ±45°) 2 top layers Foam core 3 bottom layers 0° perpendicular
Starboard	DB240 (±45°) 2 top layers Foam core 3 bottom layers 0° parallel	DBL700(0°, ±45°) 2 top layers Foam core 3 bottom layers 1 layer unidirectional 0° parallel	DB240 (±45°) 2 top layers Foam core 3 bottom layers 1 layer unidirectional 0° parallel	DBL700(0°, ±45°) 2 top layers Foam core 3 bottom layers 1 layer unidirectional 0° perpendicular	DBL700(0°, ±45°) 2 top layers Foam core 3 bottom layers 0° parallel

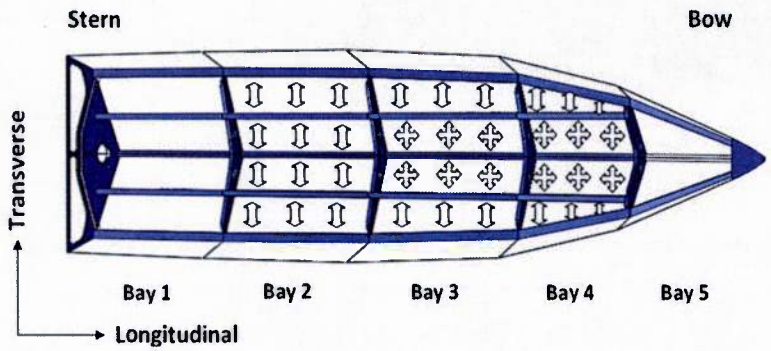

Figure 7: Boat Layout and Strain Gage Positions

Static Displacement Tests of Bottom Panels

The ratio of the port and starboard panel displacements resulting from a static load in bay 4 are shown in Figure 8. The load consisted of a number of point loads which together simulate an essentially evenly distributed pressure. Figure 8 shows the shape of the bay 4 panels and the location of relevant structure including the keel, chine, main longeron and bulkheads. The locations where displacements were measured, and the displacement ratios between port and starboard, are indicated by the arrows. The static displacement testing shows a consistent trend between the port and starboard panels in bay 4. The measurements from the six LVDT's at different locations indicate that the port panel displacements are approximately 1.6 times that of the starboard panel. The lower stiffness in the port panel is anticipated due to the orientation of fiber parallel to the longeron in the port panel as opposed to the perpendicular orientation in the starboard panel.

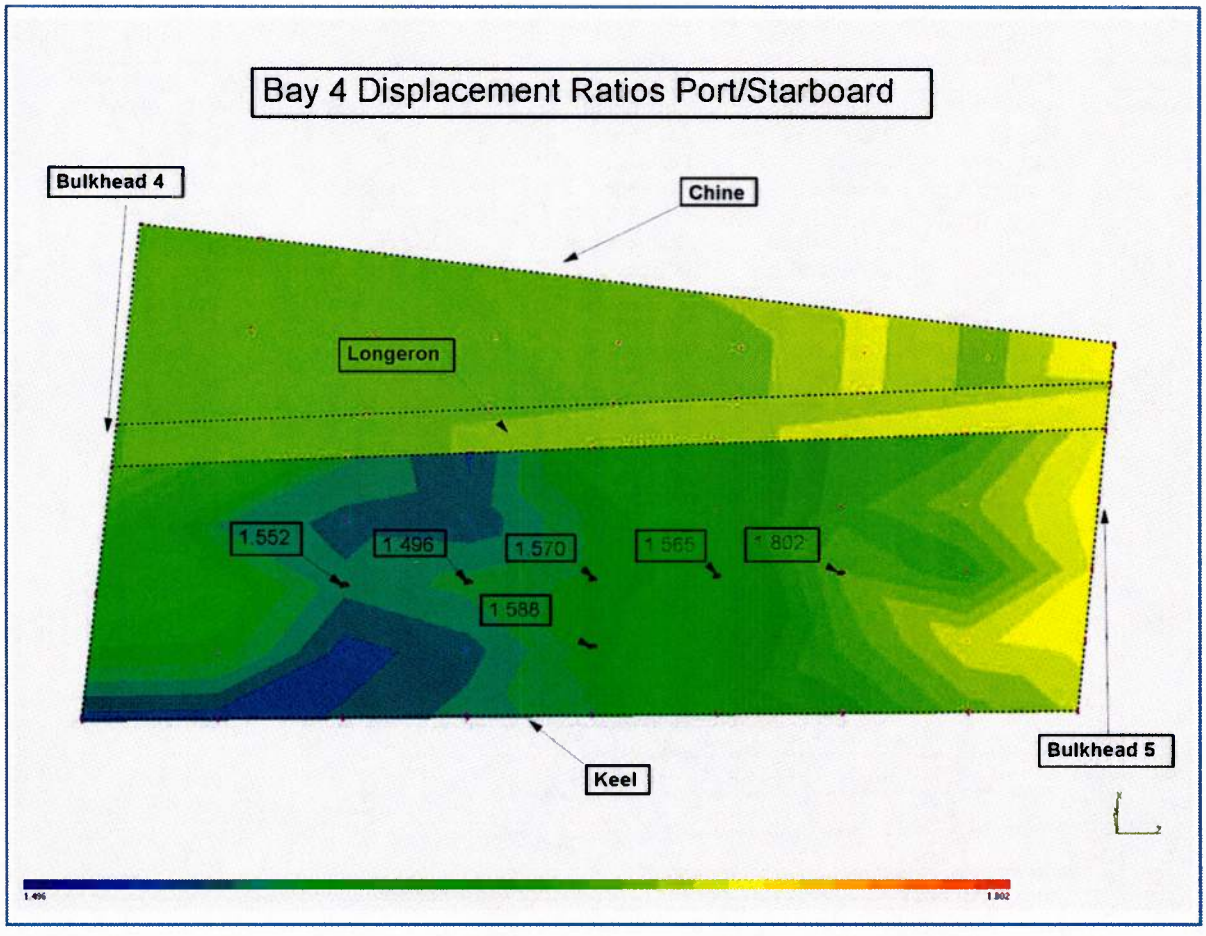

Figure 8: Relative displacement of port and starboard panels to unit distributed load at Indicated locations

The ratio of strains recorded by the inner skin gages oriented at 90 degrees show a similar result, as seen in Table 4. The strain resulting from an essentially evenly distributed load was approximately 1.6 times higher in the port panel than the starboard panel.

Table 4: Strain ratio of port and starboard panels due to distributed load

Bay 4 Port/Starboard Strain Ratios	
Front inner skin 90 degree	1.574
Middle inner skin 90 degree	1.606
Rear inner skin 90 degree	1.605

Modal Tests

Modal tests were performed wherein the free section of the bottom panels was excited with an instrumented impact hammer, and the panel response was measured with both accelerometers and strain gages. The frequency response function of the port and starboard bay 4 panels is shown in Figure 9 and Figure 10. The dominant frequency in the port panel is at 370.8 Hz, compared with 396.7 Hz in the starboard panel. Secondary peaks occur at 550.8 Hz and 563 Hz. This response spectrum is from an accelerometer mounted in the center of the panel, but is characteristic of the response from any of the accelerometer positions. The responses of strain gages on the panel inner skin indicate the same eigenfrequencies. At frequencies above the 550 Hz peaks the trend changes. In the port panel response there are peaks at 697.3 Hz and 894.2 Hz, whereas in the starboard panel there are peaks at 662.2 Hz and 851.4 Hz. Further work needs to be done in order to identify the modes related to these eigenfrequencies.

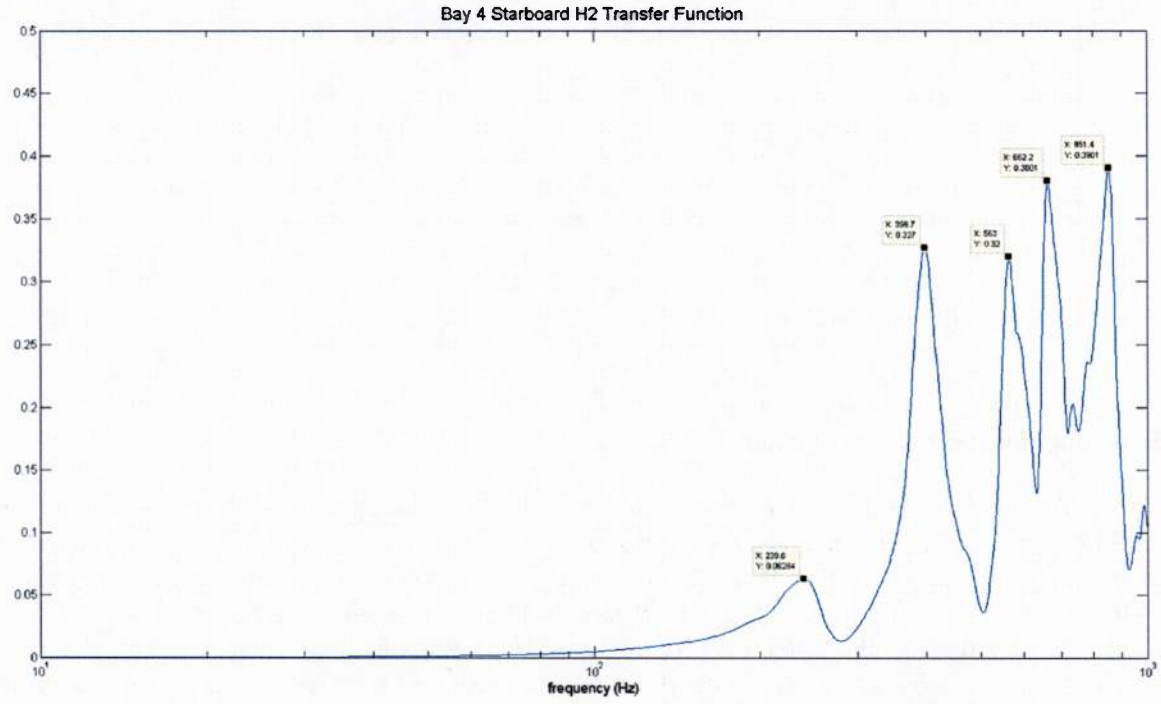

Figure 9: Bay 4 Starboard Panel Frequency Response Function

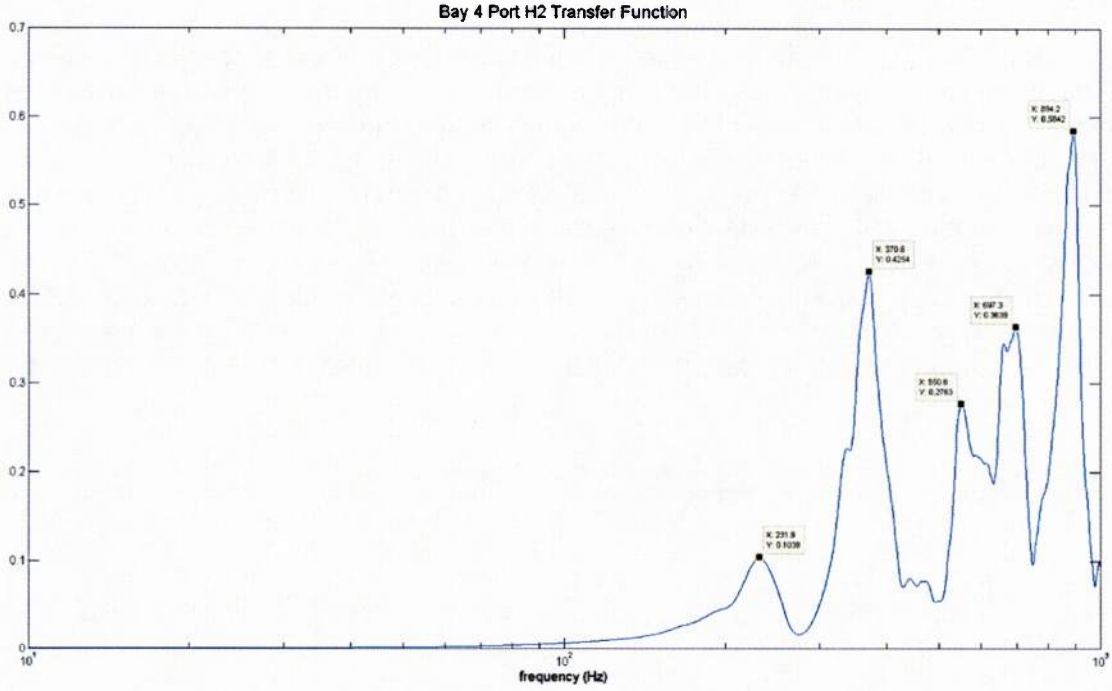

Figure 10: Bay 4 Port Panel Frequency Response Function

Slamming Time Domain Panel Strain

An isolated slamming event is shown in Figure 11. The upper plot shows 90 and 0 degree strain signals for the inner and outer skins on the port panel, while the lower plot shows the response for the starboard panel. The strains on the inner skin are in tension, while the outer skin is in compression. The largest magnitude strains are seen on the inner skin in the 90 degree direction, followed by the outer skin 90 degree. The strains in the 0 degree direction are very small compared to 90 degree strains and the results presented here will focus on the behavior of the 90 degree strains.

This slamming event is characterized by a sharp rise to peak strain, then strain drops off to a residual level and slowly decays to zero. The initial rise time is typically 10ms-20ms. In this case the initial drop off occurs around 50ms after peak strain, and the approximate duration of the decay to zero strain is an additional 200ms.

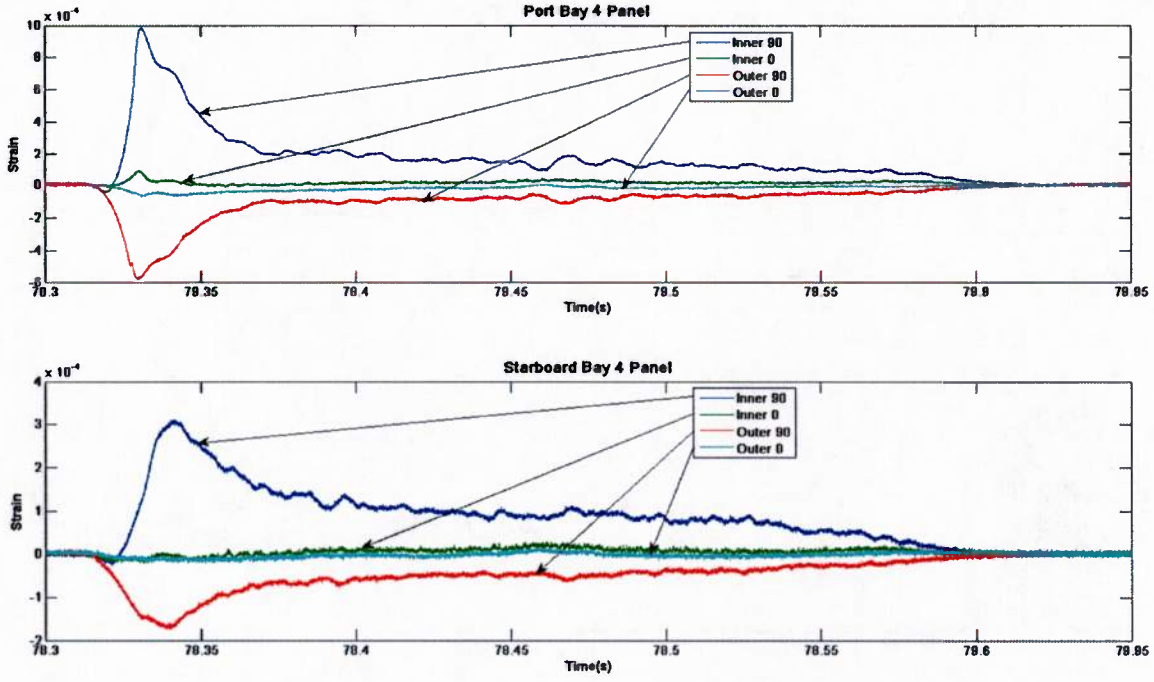

Figure 11: Strain time history in port and starboard panels during typical slamming event

Bay 4 Panel Slamming Strain Comparison

As demonstrated by the static load testing, the bay 4 port panel displacement is approximately 1.6 times greater than the bay 4 starboard panel displacement when subjected to an even pressure. The inner skin 90 degree strain is also roughly 1.6 times greater on the port panel than the starboard panel. In order to demonstrate how the slamming response is related to the static behavior, the panel strains were examined in the time domain, the frequency domain and through peak counting methods.

Figure 12 shows the 90 degree strains in the port and starboard panels during a typical slamming event, as well as the ratio of strains between the port and starboard panels versus time during the event. The port panel is subject to a large initial strain peak, with strains as much as 3 times greater than the starboard panel. Following this initial peak, the strains settle into the residual phase where the ratio is roughly 1.5-2.

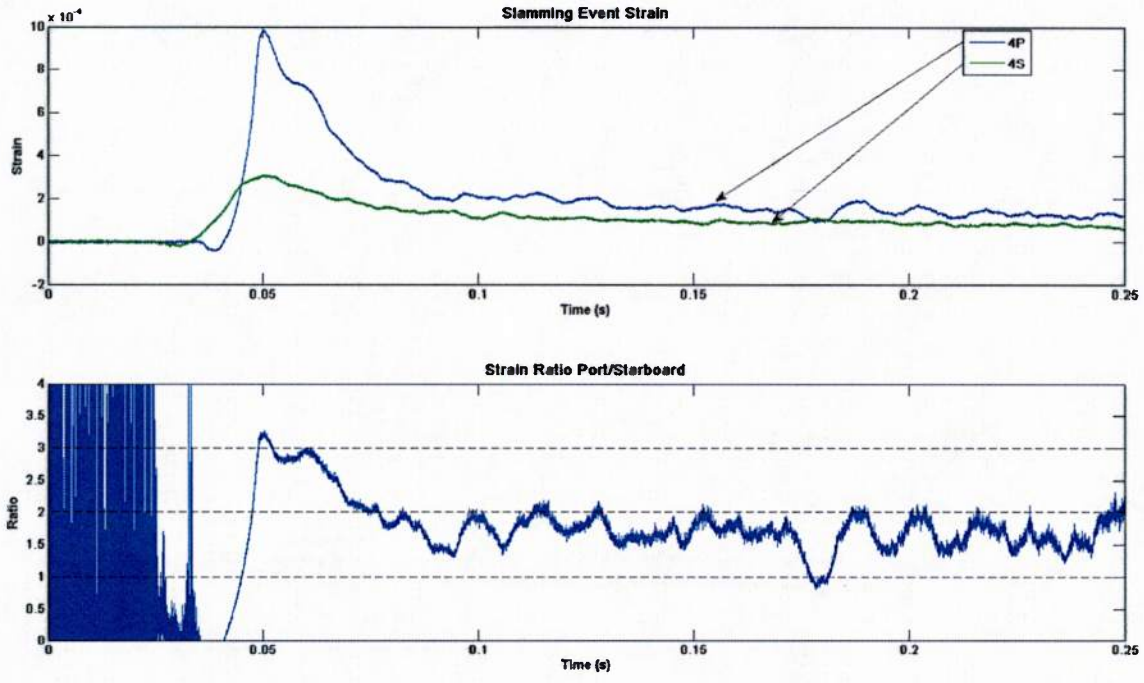

Figure 12:Port and starboard strain time histories

This time domain comparison suggests that in the residual phase of slamming the strain ratio is similar to the static case, but during the initial peak the ratio is greater. In order to further investigate this phenomenon a peak counting algorithm was used to compare the peak strains over a typical 150 second period. The peak counting algorithm used here computes the RMS value of the strain and then searches for local maxima and minima with magnitude greater than the RMS value. Slamming events during testing were typically separated by a period of approximately 1 second. To avoid counting multiple peaks from the same wave encounter the algorithm requires a minimum of 0.5 seconds between peaks. Figure 13 shows a 150 second strain time history where the peak strains found by the algorithm are identified by red triangles. Figure 14 shows the identified peak strains for gages in the two bay 4 panels sorted and plotted against each other. This plot illustrates that peak strains are consistently 2.3 times higher in the lower stiffness port panel.

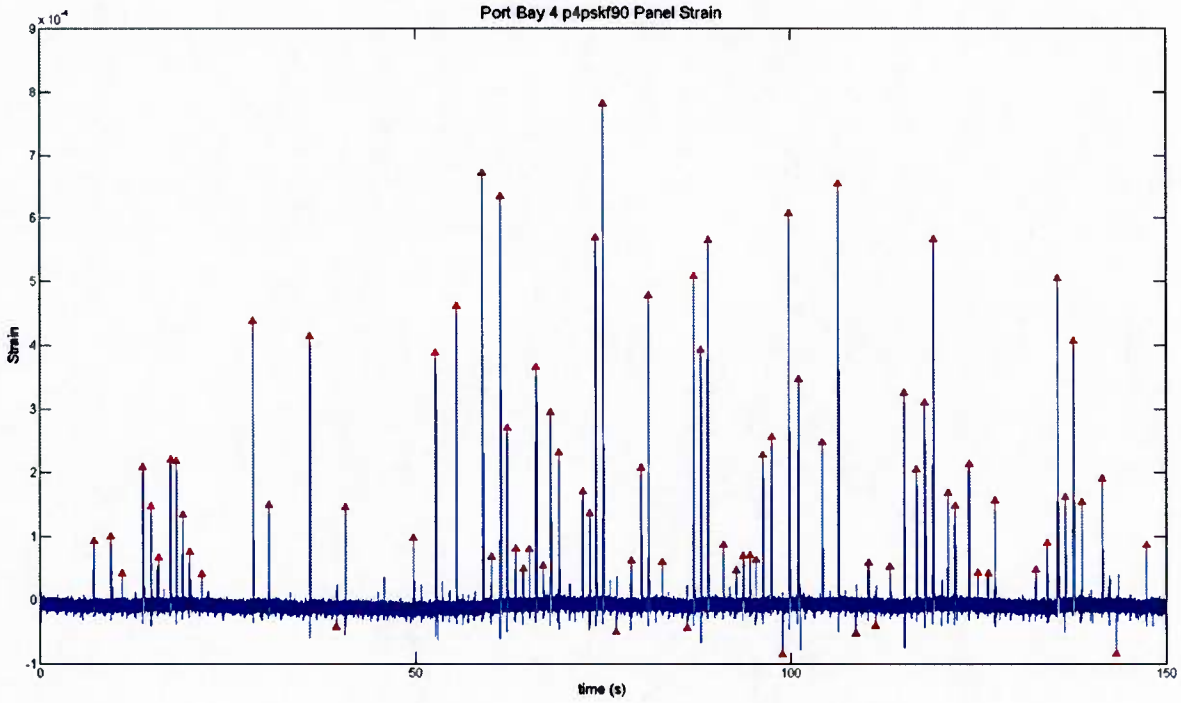

Figure 13: Panel strain time history with peaks identified

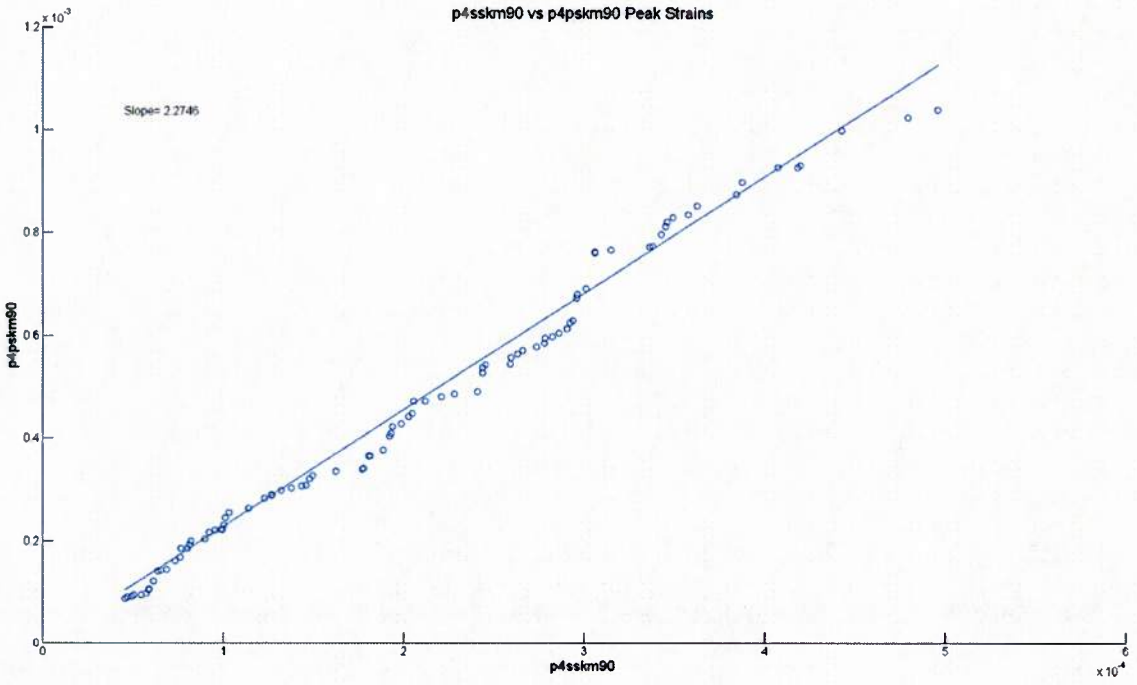

Figure 14: Port and starboard strain peaks

The third approach in characterizing the relative response of panels to slamming was to study the spectrum, or frequency content, of the responses of the bottom panels. In particular, the spectrum of the port panel divided by the spectrum of the starboard panel was studied. This has analogies with frequency response functions. Thus, the ratio of the response between port and starboard panels as a function of frequency was calculated. This frequency response function was calculated for the same 150 second period as the peak counting. Figure 15 shows that at low frequencies, the ratio of strains between the port and starboard panels is roughly 2. Between 10 and 50 Hz this ratio increases to about 2.3, the same level exhibited in the peak counting method. This frequency range is consistent with the rise time of the initial strain peak.

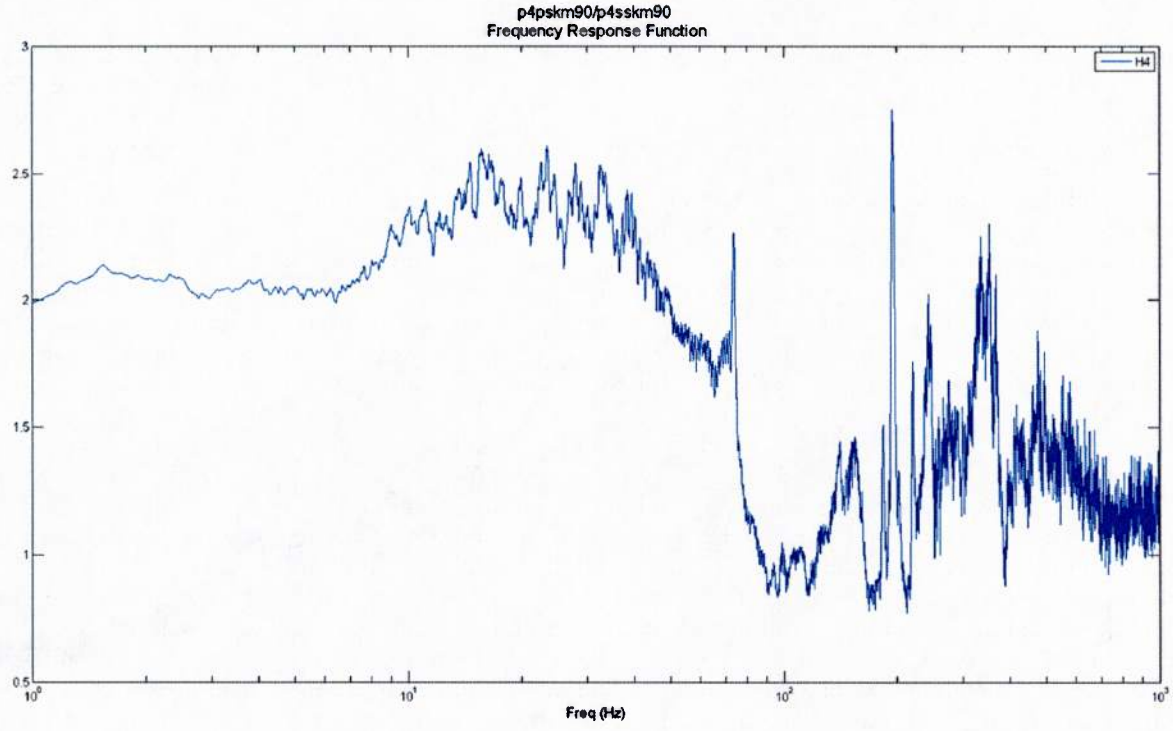

Figure 15: Port/Starboard strain frequency response function

Above 50 Hz the ratio of strains varies widely. Power spectral densities of the time signals were computed to aid in the understanding of the response in this frequency range. Figure 16 shows the power spectral densities of the port and starboard panels. The port and starboard power spectral density plots have peaks at similar frequencies. Peaks are present at 49, 73, 183, 195, 220 and 293Hz. Further investigation is needed to determine if these are so called "wet eigenfrequencies" and what effect they have on the panel behavior. The peak at 73 Hz may correspond to the engine rpm. Above 1 kHz the strain ratio is near 1, but the power spectral density indicates that at these high frequencies the amplitudes are very low and the 1:1 ratio is likely due to noise.

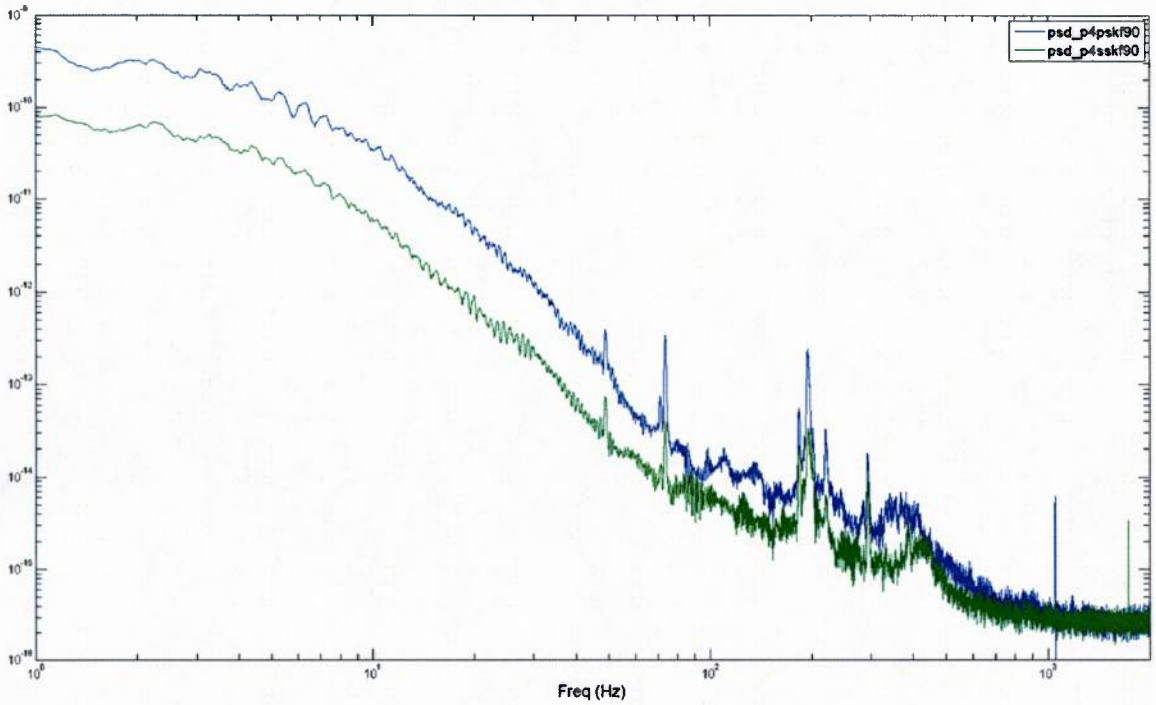

Figure 16: Port and Starboard strain power spectral densities

To further explore the panel vibration modes and the role of the wet and dry eigenfrequencies, two separate slamming modes were identified. In the first mode, illustrated in Figure 17 the vessel is rolled steeply to the port side and encounters a significant wave. The peak vertical acceleration measured at the bulkhead ahead of the bay 4 port panels was 17g. The maximum roll angle was 11 degrees. This slamming event is characterized by a brief large initial strain peak with a rise time of approximately 20ms and magnitude of 1260 microstrain on the port panel. This is followed by a lower residual strain with a longer duration. During the initial phase of the wave encounter there is a brief period of vibration at high frequency (700 Hz), possibly corresponding to the 4th "dry" eigenfrequency identified during modal testing performed on land. This is followed shortly by lower frequency vibration of approximately 73 Hz that quickly subsides. The power spectral density plots in Figure 16 show a strong peak at this frequency.

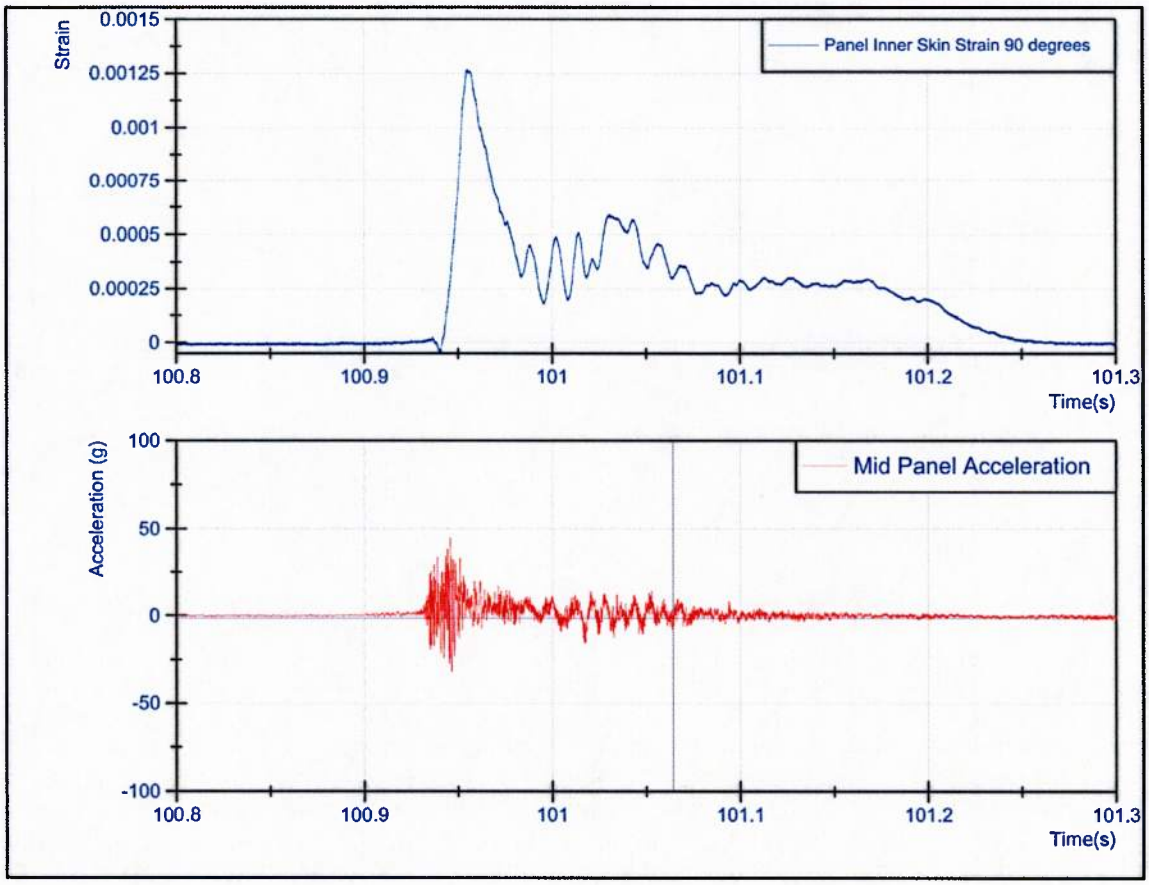

Figure 17: Strain and acceleration time history for slam mode 1

In the second slamming mode, shown in Figure 18 the vessel encounters a wave at a roll angle of 4 degrees to the port side. The maximum vertical acceleration at the bulkhead ahead of the port bay 4 panel was 7g. During this slamming event there is a single short duration strain peak reaching 750 microstrain in the port panel. This impact does not demonstrate the residual strain of the first slamming mode observed. Beginning with the initial impact, vibration is observed at 370 and 700 Hz, possibly corresponding to the second and fourth identified "dry" eigenfrequencies. No significant low frequency vibration is observed.

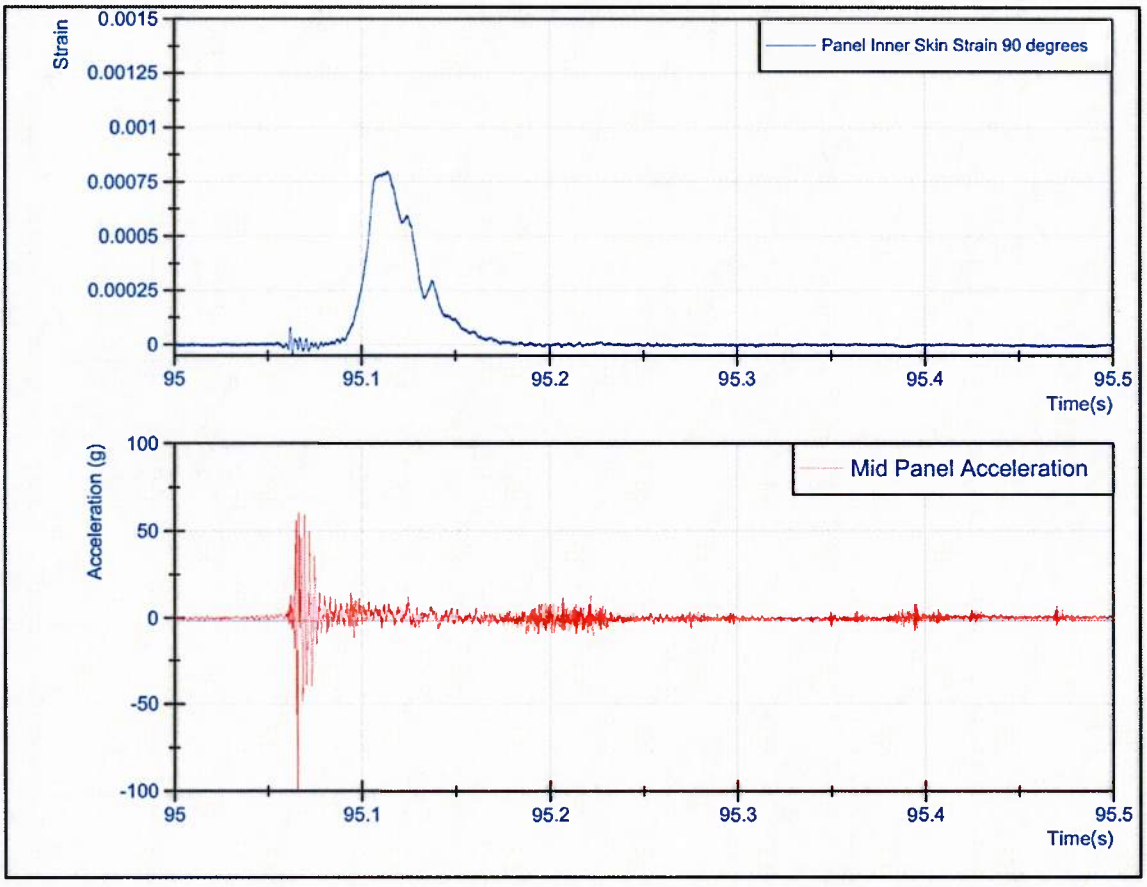

Figure 18: Strain and acceleration time history for slam mode 2

Conclusions

The data analyzed thus far for two bay 4 panels indicate that an increase in panel stiffness can result in a greater than linear decrease in panel strain during slamming events. The values for deflection and strain due to an evenly distributed static load both indicated a stiffness ratio of 1.6 between port and starboard bottom panels. During the long duration residual pressure phase of slamming, the strain data indicates a stiffness ratio of 1.5-2. Essentially the same ratio is obtained from frequency response functions computed from long time histories; they indicate that as the frequency approaches zero the strain ratio approaches 2. However, during the initial phase of slamming where the strain magnitudes are highest, the ratio is greater. Further, peak counting methods indicate strain ratios of 2.3. With rise times of 10-20ms during the initial slamming phase, the frequency response functions confirm a strain ratio of 2.3 in the corresponding 25-50 Hz range.

The influence of roll angle in slamming will be investigated further. A trim tab will be installed on the boat to allow for more control of the roll angle. Together with roll measurement provided by the

inertial navigation system a statistical study of the effect of running roll angle on rigid body motion and panel response can be performed.

Upcoming instrumentation upgrades will allow for further understanding of the slamming excitation and panel response. The addition of pressure sensing arrays on the hull will make it possible to determine the pressures on the panels and thus directly compute response functions of bottom panels. The addition of LVDTs will enable more complete understanding of deformation modes.

The role of "wet eigenfrequencies" in slamming is ongoing and will be investigated further. Vibrations at repeatable frequencies significantly lower than any of the dry eigenfrequencies have been observed. These vibrations appear to only be excited by certain types of slamming and during certain phases of the impact. The vibration modes, severity and their effect on the panels are not yet understood. Further work will correlate the experimental data with recent analytical work on slamming.